
STRUCTURE, PHASE TRANSFORMATIONS,
AND DIFFUSION

The Influence of Frictional Treatment and Low-Temperature Plasma Carburizing on the Structure and Phase Composition of Metastable Austenitic Steel

R. A. Savrai^{a, *}, P. A. Skorynina^a, A. V. Makarov^{a, b}, A. I. Men'shakov^{c, d}, and V. S. Gaviko^b

^a Institute of Engineering Science, Ural Branch, Russian Academy of Sciences, Ekaterinburg, 620049 Russia

^b Mikheev Institute of Metal Physics, Ural Branch, Russian Academy of Sciences, Ekaterinburg, 620108 Russia

^c Institute of Electrophysics, Ural Branch, Russian Academy of Sciences, Ekaterinburg, 620016 Russia

^d Ural Federal University Named after the First President of Russia B.N. Yeltsin, Ekaterinburg, 620002 Russia

*e-mail: ras@imach.uran.ru

Received January 2, 2023; revised March 20, 2023; accepted March 29, 2023

Abstract—The features of the structure and phase composition of corrosion-resistant austenitic chromium–nickel steel (16.80 wt % Cr, 8.44 wt % Ni) subjected to carburizing in electron beam plasma at temperatures of 350 and 500°C, frictional treatment with a sliding indenter, and a combination of frictional treatment and plasma carburizing have been considered. It has been established that plasma carburizing results in the formation of a modified surface layer consisting of carbon-saturated austenite and carbides (Cr_{23}C_6 , Fe_3C); in this case, the formation of γ_{C} -phase occurs only at a temperature of 350°C. The depth of a modified layer increases with an increase in the carburizing temperature. It has been shown that it is useful to perform combined frictional treatment and plasma carburizing at a carburizing temperature of 350°C, since in this case the deformation-induced structure formed as a result of frictional treatment is preserved, and the precipitated carbides remain highly dispersed. In this case, frictional treatment should provide the formation of the deepest possible diffusion-active layer with a dispersed structure.

Keywords: corrosion-resistant austenitic steel, plasma carburizing, frictional treatment, structure, phase composition

DOI: 10.1134/S0031918X23600483

INTRODUCTION

There are many ways to harden the surface of austenitic steels. Surface deformation treatments and various types of chemical surface modification are the most widely used. Frictional treatment [1–8] can be highlighted among the methods of strain hardening of austenitic steels that are prone to adhesion upon contact interaction. Together with efficient hardening, frictional treatment of austenitic steels makes it possible to obtain high-quality low-roughness surfaces with negligible amount of material-continuity defects. In this case, the depth of the hardened layer can reach 500 μm . Among the known methods of chemical modification, low-temperature (below 550°C) plasma surface treatments are of great interest, in particular, plasma carburizing [9–16] and plasma nitriding [17–19]. These plasma treatments make it possible to obtain austenite in the steel structure supersaturated with carbon (γ_{C}) or nitrogen (γ_{N}) with increased hardness, which contributes to effective hardening and improving the service characteristics of austenitic chromium–nickel steels. However, as a rule, the depth of the hardened

layer does not exceed 100 μm . It should be noted that plasma carburizing and nitriding are usually performed using glow discharge facilities. However, there are alternative ways to generate plasma. For example, the use of low-energy electron beams [16, 17] makes it possible to efficiently generate high-density plasma (10^{10} – 10^{12} cm^{-3}) and obtain a required temperature of treated objects with no use of external heating, which is a significant advantage.

The attention of researchers to combined treatments including strain hardening and chemical modification of the steel surface has significantly increased in recent years [20–29]. In particular, this makes it possible to obtain a higher depth of hardening with a higher quality of the hardened surface. For example, the use of frictional treatment before plasma nitriding makes it possible to reduce the roughness parameter Ra of the formed surface of austenitic steel by several times [26]. It should be emphasized that there is no information in the literature on the use of combined treatment of austenitic chromium–nickel steels, which includes carburizing in electron beam plasma with preliminary frictional treatment. Thus, the use of

this combined treatment is not only practically substantiated, but is also of considerable scientific interest.

The aim of this work was to study the structure and phase composition of austenitic AISI 321 steel subjected to carburizing in electron beam plasma at temperatures of 350 and 500°C, to frictional treatment with a sliding indenter, and to combined frictional treatment and plasma carburizing.

EXPERIMENTAL

The material under study was commercial corrosion-resistant austenitic AISI 321 steel with the following chemical composition (wt %): 0.05 C, 16.80 Cr, 8.44 Ni, 0.33 Ti, 1.15 Mn, 0.67 Si, 0.26 Mo, 0.13 Co, 0.03 Nb, 0.31 Cu, 0.036 P, 0.005 S, and Fe for balance. The studied samples of 40 × 25 × 10 mm were cut out from sheet steel using electroerosive cutting on a FANUC Robocut α -0iE machine. Before subsequent treatment, the samples were subjected to quenching from 1100°C with water cooling, mechanical grinding, and electrolytic polishing in sulfur-phosphorus electrolyte with the composition 100 mL H₂SO₄ + 400 mL H₃PO₄ + 20 g CrO₃. The prepared samples were subjected to frictional treatment, plasma carburizing, or combined treatments, as a result of which a set of studied samples was obtained (Table 1).

Carburizing of samples was performed in argon-acetylene (Ar + C₂H₂) plasma of a low-energy electron beam. A two-stage source of a wide electron beam ($D = 100$ mm) with a meshed plasma cathode was used. Figure 1 shows the experimental setup for carburizing. At the initial stage, a glow discharge was ignited in an argon atmosphere (30 cm³/min), then an accelerating voltage (U_2) was applied between the mesh and discharge chamber. A bias voltage (−350 V relative to the discharge chamber) was applied to the table with the samples, and the samples were subjected to ion purification and heating for 30 min. Next, acetylene (1.5 cm³/min) was let into the chamber and the beam parameters were set (current I_2 , voltage U_2), which provided heating of the samples to the required temperature ($T = 350$ and 500°C). The samples were held in the steady state for 6 h. The main technological parameters of carburizing are presented in Table 2.

The frictional treatment of samples was performed using a laboratory setup in an oxidation-free argon-flow medium with reciprocating sliding of a semi-spherical indenter made of synthetic diamond with semi-sphere radius $R = 3$ mm along the steel surface at the average sliding speed $V = 0.065$ m/s under the load $P = 392$ N and single scanning of the sample surface with indenter displacement $d = 0.1$ mm for each double pass.

The structure of AISI 321 steel after different treatment modes was studied using a Tescan VEGA II XMU scanning electron microscope (SEM). X-ray dif-

Table 1. Treatment modes of AISI 321 steel

Sample no.	Treatment mode
1	Quenching (HT)
2	Plasma carburizing at $T = 350^\circ\text{C}$ (PC350)
3	Plasma carburizing at $T = 500^\circ\text{C}$ (PC500)
4	Frictional treatment (FT)
5	Frictional treatment + plasma carburizing at $T = 350^\circ\text{C}$ (CT350)
6	Frictional treatment + plasma carburizing at $T = 500^\circ\text{C}$ (CT500)

Table 2. Plasma carburizing modes of AISI 321 steel (T is the heating temperature, I_2 is the beam current, U_2 is the accelerating voltage, J_1 is the ion current density)

T , °C	I_2 , A	U_2 , V	J_1 , mA/cm ²
350	2.9	200	3.4
500	4.3	310	5.0

fraction (XRD) analysis was performed on a PANalytical Empyrean diffractometer in CuK α radiation. The phase composition, angular position 2θ of lines, and integral width B of lines were determined.

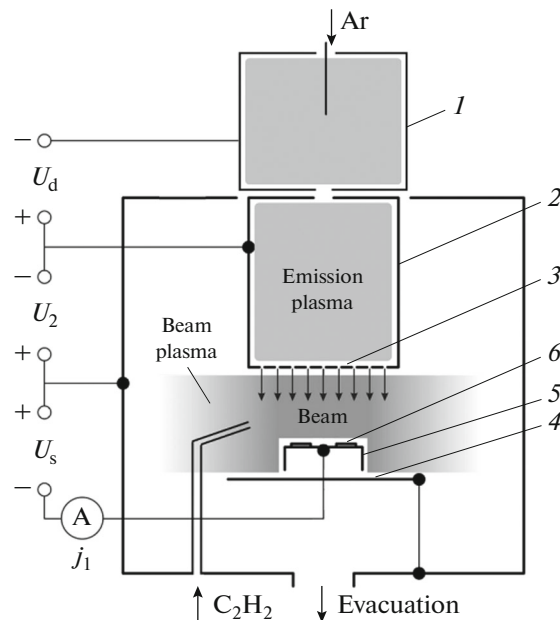


Fig. 1. The experimental setup for carburizing: (1) hollow cathode, (2) hollow anode, (3) mesh of the plasma anode, (4) samples, (5) isolated table, and (6) collector.

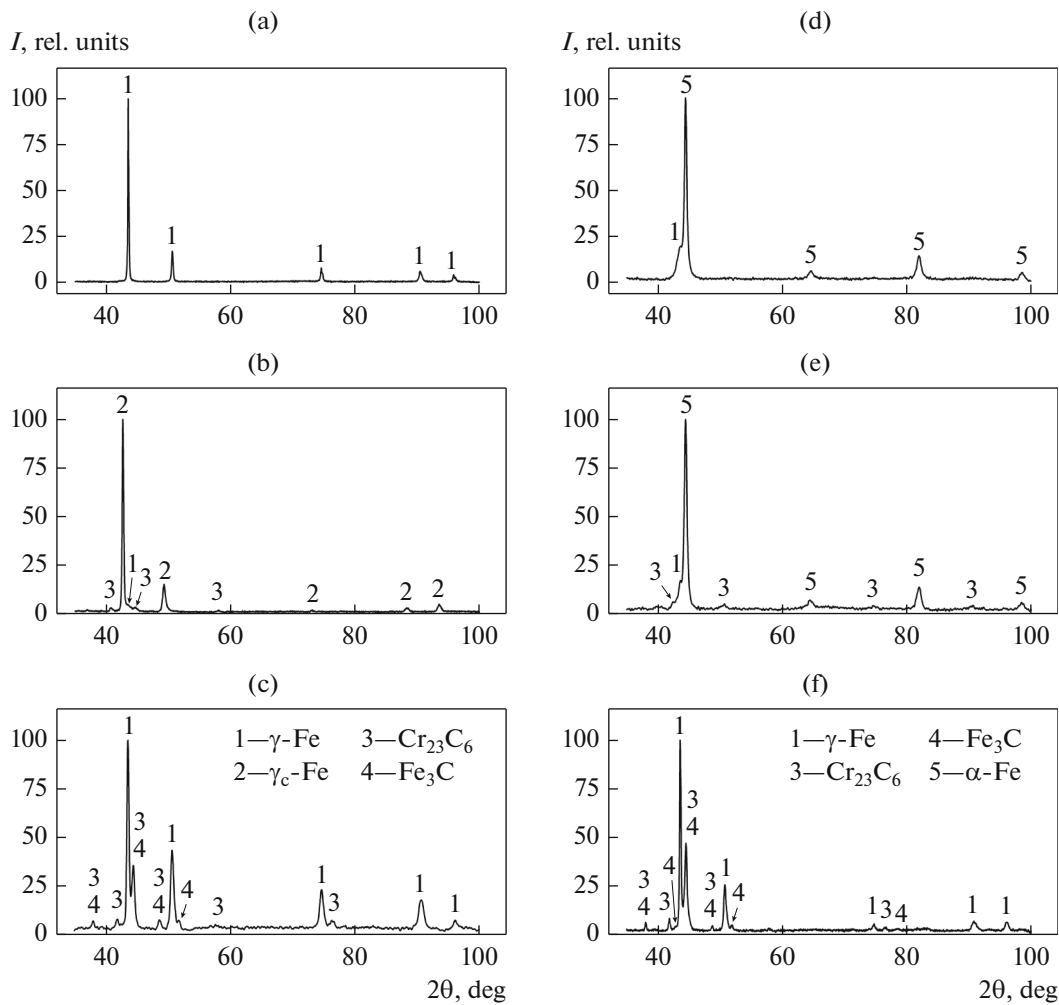


Fig. 2. X-ray diffraction patterns of the surface of AISI 321 steel: (a) after quenching, after plasma carburizing at temperature T of (b) 350 and (c) 500°C, (d) after surface frictional treatment, after frictional treatment and plasma carburizing at temperature T of (e) 350 and (f) 500°C.

RESULTS AND DISCUSSION

The microstructure of quenched AISI 321 steel is fully austenitic with the titanium carbide TiC inclusions [2, 7, 30, 31]. XRD analysis showed that there is no α phase in the structure of quenched steel (Fig. 2a, Table 3). After plasma carburizing at a temperature $T = 350^\circ\text{C}$, a 25 μm -thick modified layer is formed on the surface of AISI 321 steel, which is clearly seen on the transverse section (Fig. 3a). The presence of this layer is commonly related to the formation of carbon-supersaturated austenite γ_{C} [11], which is confirmed by the XRD data (Fig. 2b, Table 3). These data show that after carburizing at $T = 350^\circ\text{C}$, the maxima of austenite lines are shifted towards smaller diffraction angles, i.e., the γ_{C} phase with an increased lattice parameter a_{γ} is formed. The determination of carbon content X_{C} in the γ_{C} phase using the dependence $a_{\gamma} = a_0 + 0.044X_{\text{C}}$ [32] (where $a_0 = 3.607 \text{ \AA}$, $a_{\gamma} = 3.668 \text{ \AA}$) resulted in $X_{\text{C}} = 1.39 \text{ wt \%}$. Carburizing at $T = 350^\circ\text{C}$

also results in the formation of chromium carbide Cr_{23}C_6 . Precipitation of carbides leads to depletion of neighboring austenite regions of carbon, which is confirmed by a weak peak of the γ phase in the diffraction pattern (Fig. 2b). It is important to emphasize that the precipitation of secondary phases in the AISI 321 steel was previously observed upon chemical modification of the surface with similar parameters (temperature and holding time) [23, 28]. In particular, the formation of Cr–N and Fe–N chemical bonds after plasma nitriding at $T = 350^\circ\text{C}$ was shown for the first time in [28] using X-ray photoelectron spectroscopy (XPS).

An increase in the plasma carburizing temperature to $T = 500^\circ\text{C}$ results in a depth of the modified layer of at least 45–50 μm due to enhanced diffusion of carbon into the steel surface at a higher treatment temperature (Fig. 3b); however, the layer is not as pronounced as after carburizing at $T = 350^\circ\text{C}$ (Fig. 3a). A large number of dispersed particles are observed within this layer

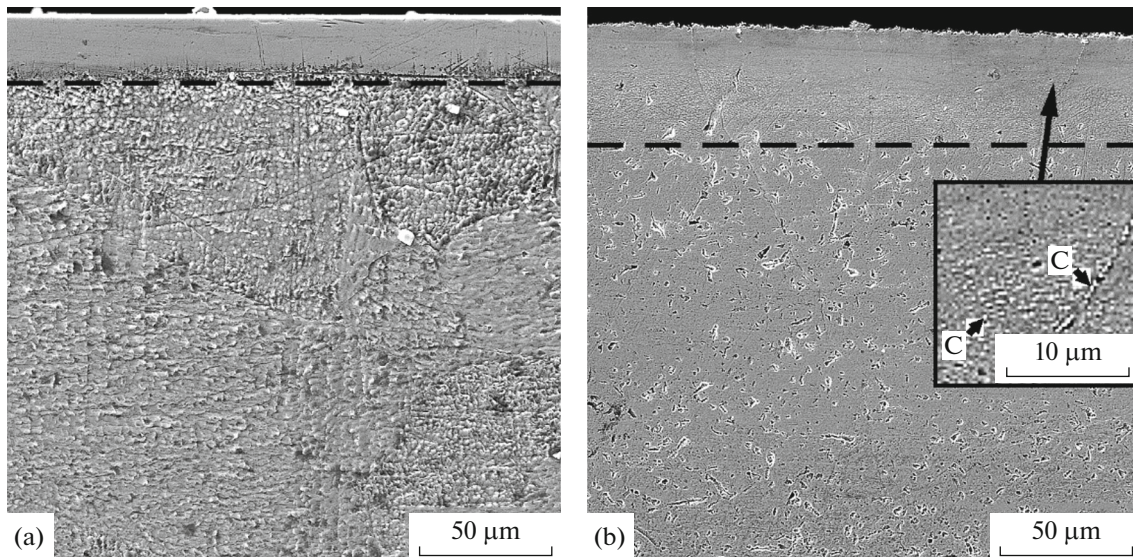


Fig. 3. SEM images of the structure of the surface layer of AISI 321 steel after plasma carburizing at temperature T of (a) 350 and (b) 500°C Arrows “C” indicate carbides.

(Fig. 3b), which, according to XRD, are chromium carbide Cr_{23}C_6 and cementite Fe_3C (Fig. 2c). The formation of carbides leads to a shift of the maxima of the austenite lines towards larger diffraction angles (Table 3) and to a decrease in the carbon content in austenite, as a result of which the γ_{C} phase is not formed. We note that the integral width $B_{(111)\gamma}$ of the X-ray line of austenite increases with an increase in the plasma carburizing temperature. The increase in the line width is caused by crystal lattice microdistortions, which can be caused by both the increased carbon content in the lattice and the growth in the density of crystal structure defects due to relaxation of thermal stresses by deformation upon cooling after carburizing [30, 31]. An increase in the carburizing temperature leads to an increase in thermal stresses; therefore, after carburizing at $T = 500^\circ\text{C}$, the width $B_{(111)\gamma}$ is slightly larger than

after carburizing at $T = 350^\circ\text{C}$ (Table 3), even despite the lower carbon content in austenite after carburizing at $T = 500^\circ\text{C}$.

The frictional treatment results in the formation of a 20–25 μm -thick deformed layer on the surface of AISI 321 steel containing elongated crystals (Fig. 4). At a depth of more than 25 μm , a structure of deformed austenite is observed with a large number of slip bands within the initial austenite grains (Fig. 4). According to the data of X-ray diffraction analysis, frictional treatment is accompanied by the formation of deformation-induced martensite in the surface layer of the AISI 321 steel in the amount of $V_{\alpha} = 72 \text{ vol } \%$, as well as a sharp increase in the width $B_{(111)\gamma}$ from 16.0 to 100.7 min and a shift of the maxima of austenite lines towards larger diffraction angles as a result of an intensive deformation effect on the treated surface (Fig. 2d, Table 3).

Table 3. The volume contents V_{α} and V_{γ} of α and γ phases, diffraction angle 2θ of X-ray lines $(111)\gamma$ and $(110)\alpha$, integral width B of X-ray lines $(111)\gamma$ and $(110)\alpha$ in the surface layer of AISI 321 steel after different treatment modes

Treatment mode	V_{γ} , vol %	V_{α} , vol %	$2\theta_{(111)\gamma}$, deg	$2\theta_{(110)\alpha}$, deg	$B_{(111)\gamma}$, min	$B_{(110)\alpha}$, min
HT	100	—	43.55	—	16.0	—
PC350	100	—	42.69	—	17.3	—
PC500	100	—	43.62	—	22.2	—
FT	28	72	43.72	44.48	100.7	37.3
CT350	28	72	43.67	44.48	78.0	40.9
CT500	100	—	43.60	—	16.6	—

Note. The volume contents V_{α} and V_{γ} are given without taking into account the content of carbide phase.

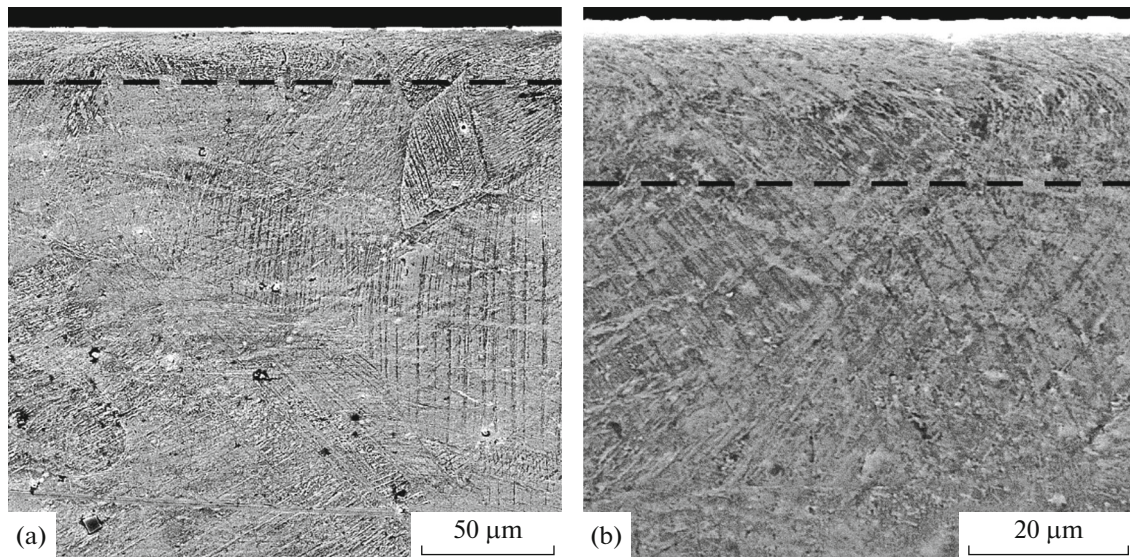


Fig. 4. SEM images of the structure of the surface layer of AISI 321 steel after frictional treatment.

The combined treatment, including frictional treatment and plasma carburizing at a temperature of $T = 350^\circ\text{C}$, is accompanied by the precipitation of dispersed particles in the surface layer of steel (Figs. 5a, 5b), which are chromium carbide Cr_{23}C_6 (Fig. 2e). We note that carbides are observed at a depth less than $25\ \mu\text{m}$, i.e., the highest diffusion activity is exhibited by the layer with a highly dispersed structure. Therefore, frictional treatment should provide the formation of the deepest possible diffusion-active layer. The amount of the α phase after such a combined treatment does not decrease and is preserved at a level of $V_\alpha = 72\ \text{vol}\ \%$, but the width $B_{(110)\alpha}$ increases from 37.3 to 40.9 min (see Table 3). Taking the defect structure of deformation-induced martensite into account, the indicated increase in the width $B_{(110)\alpha}$ can be due to the saturation of the α phase with carbon in the course of carburizing. The width $B_{(111)\gamma}$, on the contrary, decreased from 100.7 to 78.0 min (Table 3), which may be due to the recovery in cold-worked austenite when heating in the course of carburizing.

The combined treatment including frictional treatment and plasma carburizing at a temperature of $T = 500^\circ\text{C}$ was accompanied by the precipitation of a higher amount of larger particles in a 20–25 μm thick layer; the number of these particles in the underlying layers was considerably less (Figs. 5c, 5d). According to the XRD analysis, these particles are chromium carbide Cr_{23}C_6 and cementite Fe_3C (Fig. 2f). In this case, there is no α phase in the steel structure, and the width $B_{(111)\gamma}$ sharply decreased from 78.0 to 16.6 min and became almost equal to the width of the quenched-steel line (Fig. 2f, Table 3), which indicates that recrystallization occurred. We note that the combined treatment does not significantly affect the posi-

tion of the maxima of the α -phase lines; the maxima of the austenite lines shift towards smaller angles with increasing carburizing temperature and come close to the positions of the maxima of the quenched-steel lines (Table 3) due to the recovery in cold-worked austenite and recrystallization.

CONCLUSIONS

The structure and phase composition of the austenitic AISI 321 steel subjected to frictional treatment and carburizing in electron beam plasma at temperatures $T = 350$ and 500°C have been studied.

It has been established that plasma carburizing results in the formation of a modified surface layer consisting of the carbon-enhanced austenite and carbides. The phase composition after carburizing at $T = 350$ and 500°C can be determined as $\gamma_C + \gamma + \text{Cr}_{23}\text{C}_6$ and $\gamma + \text{Cr}_{23}\text{C}_6 + \text{Fe}_3\text{C}$, respectively. The depth of the modified layer grows with an increase in the carburizing temperature and is $25\ \mu\text{m}$ at $T = 350^\circ\text{C}$ and no less than 40–45 μm at $T = 500^\circ\text{C}$.

Frictional treatment results in the formation of a deformation-induced austenitic–martensitic structure in the surface layer of the AISI 321 steel. The phase composition after the combined treatment including frictional treatment and carburizing at $T = 350$ and 500°C can be determined as $\alpha' + \gamma + \text{Cr}_{23}\text{C}_6$ and $\gamma + \text{Cr}_{23}\text{C}_6 + \text{Fe}_3\text{C}$, respectively.

It has been shown that it is useful to perform the combined frictional treatment and plasma carburizing at a carburizing temperature $T = 350^\circ\text{C}$, since in this case the deformation-induced structure formed as a result of frictional treatment is preserved and the precipitated carbides remain highly dispersed. In this

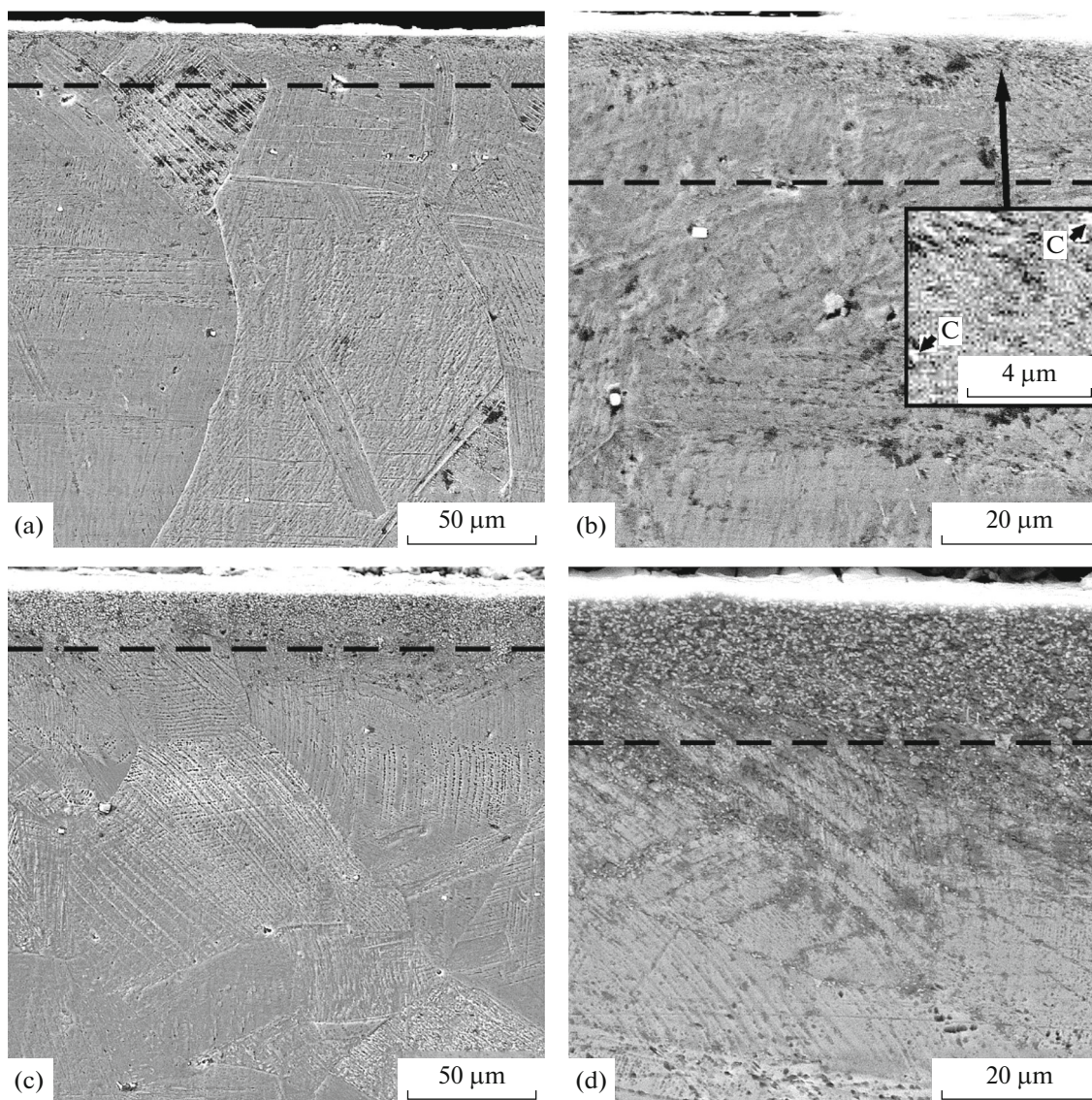


Fig. 5. SEM images of the structure of the surface layer of AISI 321 steel after frictional treatment and plasma carburizing at temperature T of (a, b) 350 and (c, d) 500°C. Arrows “C” indicate carbides.

case, frictional treatment should provide the formation of the deepest possible diffusion-active layer with a dispersed structure.

ACKNOWLEDGMENTS

Electron scanning microscopy was performed at the Plastometriya Center of the Collaborative Access at the Institute of Engineering Science, Ural Branch, Russian Academy of Sciences.

FUNDING

This work was performed within the framework of the state tasks of the Institute of Engineering Science, Ural Branch, Russian Academy of Sciences (theme no. AAAA-

A18-118020790147-4), the Institute of Metal Physics, Ural Branch, Russian Academy of Sciences (Structure theme no. 122021000033-2), and the Institute of Electrophysics, Ural Branch, Russian Academy of Sciences (theme no. 122011200365-3).

CONFLICT OF INTEREST

The authors declare that they have no conflicts of interest.

OPEN ACCESS

This article is licensed under a Creative Commons Attribution 4.0 International License, which permits use, sharing, adaptation, distribution and reproduction in any medium or format, as long as you give appropriate credit to the original

author(s) and the source, provide a link to the Creative Commons license, and indicate if changes were made. The images or other third party material in this article are included in the article's Creative Commons license, unless indicated otherwise in a credit line to the material. If material is not included in the article's Creative Commons license and your intended use is not permitted by statutory regulation or exceeds the permitted use, you will need to obtain permission directly from the copyright holder. To view a copy of this license, visit <http://creativecommons.org/licenses/by/4.0/>.

REFERENCES

1. A. V. Makarov, P. A. Skorynina, A. S. Yurovskikh, and A. L. Osintseva, "Effect of the conditions of the nanostructuring frictional treatment process on the structural and phase states and the strengthening of metastable austenitic steel," *Phys. Met. Metallogr.* **118**, 1225–1235 (2017).
<https://doi.org/10.1134/S0031918X17120092>
2. R. A. Savrai, A. V. Makarov, I. Yu. Malygina, S. A. Rogovaya, and A. L. Osintseva, "Improving the strength of the AISI 321 austenitic stainless steel by frictional treatment," *Diagn., Resour. Mech. Mater. Struct.*, No. 5, 43–62 (2017).
<https://doi.org/10.17804/2410-9908.2017.5.043-062>
3. N. A. Narkevich, I. A. Shulepov, and Yu. P. Mironov, "Structure, mechanical, and tribotechnical properties of an austenitic nitrogen steel after frictional treatment," *Phys. Met. Metallogr.* **118**, 399–406 (2017).
<https://doi.org/10.1134/S0031918X17020090>
4. A. V. Makarov and L. G. Korshunov, "Metallophysical foundations of nanostructuring frictional treatment of steels," *Phys. Met. Metallogr.* **120**, 303–311 (2019).
<https://doi.org/10.1134/S0031918X18120128>
5. A. V. Makarov, P. A. Skorynina, E. G. Volkova, and A. L. Osintseva, "Effect of heating on the structure, phase composition, and micromechanical properties of the metastable austenitic steel strengthened by nanostructuring frictional treatment," *Phys. Met. Metallogr.* **119**, 1196–1203 (2018).
<https://doi.org/10.1134/S0031918X18120116>
6. A. V. Makarov, R. A. Savrai, P. A. Skorynina, and E. G. Volkova, "Development of methods for steel surface deformation nanostructuring," *Met. Sci. Heat Treat.* **62**, 61–69 (2020).
<https://doi.org/10.1007/s11041-020-00513-4>
7. R. A. Savrai and A. L. Osintseva, "Effect of hardened surface layer obtained by frictional treatment on the contact endurance of the AISI 321 stainless steel under contact gigacycle fatigue tests," *Mater. Sci. Eng., A* **802**, 140679 (2021).
<https://doi.org/10.1016/j.msea.2020.140679>
8. R. A. Savrai, Yu. M. Kolobylin, and E. G. Volkova, "Micromechanical characteristics of the surface layer of metastable austenitic steel after frictional treatment," *Phys. Met. Metallogr.* **122**, 800–806 (2021).
<https://doi.org/10.1134/S0031918X21080123>
9. Y. Sun, X. Li, and T. Bell, "Structural characteristics of low temperature plasma carburised austenitic stainless steel," *Mater. Sci. Technol.* **15**, 1171–1178 (1999).
<https://doi.org/10.1179/026708399101505077>
10. Y. Sun, "Kinetics of low temperature plasma carburizing of austenitic stainless steels," *J. Mater. Process. Technol.* **168**, 189–194 (2005).
<https://doi.org/10.1016/j.jmatprotec.2004.10.005>
11. R. M. Souza, M. Ignat, C. E. Pinedo, and A. P. Tschiptschin, "Structure and properties of low temperature plasma carburized austenitic stainless steels," *Surf. Coat. Technol.* **204**, 1102–1105 (2009).
<https://doi.org/10.1016/j.surfcoat.2009.04.033>
12. Y. Sun, "Tribocorrosion behavior of low temperature plasma carburized stainless steel," *Surf. Coat. Technol.* **228**, S342–S348 (2013).
<https://doi.org/10.1016/j.surfcoat.2012.05.105>
13. X. Tong, T. Zhang, and W. Ye, "Effect of carburizing atmosphere proportion on low temperature plasma carburizing of austenitic stainless steel," *Appl. Mech. Mater.* **598**, 90–93 (2014).
<https://doi.org/10.4028/www.scientific.net/amm.598.90>
14. M. C. S. Duarte, C. Godoy, and J. C. Avelar-Batista Wilson, "Analysis of sliding wear tests of plasma processed AISI 316L steel," *Surf. Coat. Technol.* **260**, 316–325 (2014).
<https://doi.org/10.1016/j.surfcoat.2014.07.094>
15. R. L. Liu, S. Wang, C. Y. Wei, M. F. Yan, and Y. J. Qiao, "Microstructure and corrosion behavior of low temperature carburized AISI 304 stainless steel," *Mater. Res. Express* **6**, 066417 (2019).
<https://doi.org/10.1088/2053-1591/ab104c>
16. P. A. Skorynina, A. V. Makarov, A. I. Men'shakov, and A. L. Osintseva, "Effect of low-temperature carburization in electron beam plasma on the hardening and surface roughness of the metastable austenitic steel," *Obrab. Met. (Tekhnol., Oborud., Instrum., No. 2)*, 97–109 (2019).
<https://doi.org/10.17212/1994-6309-2019-21.2-97-109>
17. Gavrillov N. V., Menshakov A. I., "Low temperature nitriding of stainless steel in electron beam plasma at 400°C," *Fiz. i Him. Obrab. Mater.*, No. 5, 31–36 (2012).
18. E. de Araújo Jr., R. M. Bandeira, M. D. Manfrinato, J. A. Moreto, R. Borges, S. dos Santos Vales, P. A. Suzuki, and L. S. Rossino, "Effect of ionic plasma nitriding process on the corrosion and micro-abrasive wear behavior of AISI 316L austenitic and AISI 470 super-ferritic stainless steels," *J. Mater. Res. Technol.* **8**, 2180–2191 (2019).
<https://doi.org/10.1016/j.jmrt.2019.02.006>
19. L. F. Spevak, O. A. Nefedova, A. V. Makarov, and G. V. Samoilova, "Mathematical modelling of plasma nitriding of austenitic stainless steel," *Diagn., Resour. Mech. Mater. Struct.*, No. 6, 68–79 (2015).
<https://doi.org/10.17804/2410-9908.2015.6.068-079>
20. Yi. Lin, J. Lu, L. Wang, T. Xu, and Q. Xue, "Surface nanocrystallization by surface mechanical attrition treatment and its effect on structure and properties of plasma nitrided AISI 321 stainless steel," *Acta Mater.* **54**, 5599–5605 (2006).
<https://doi.org/10.1016/j.actamat.2006.08.014>
21. M. Jayalakshmi, P. Huilgol, B. B. Ramachandra, and B. K. Udaya, "Microstructural characterization of low temperature plasma-nitrided 316L stainless steel surface with prior severe shot peening," *Mater. Des.* **108**, 448–454 (2016).
<https://doi.org/10.1016/j.matdes.2016.07.005>

22. V. A. Shabashov, L. G. Korshunov, A. V. Litvinov, N. V. Kataeva, and A. E. Zamatovsky, "Increasing the depth of the nitrided layer in the surface of austenitic alloys using friction treatment," *Diagn., Resour. Mech. Mater. Struct.*, No. 6, 17–27 (2016).
<https://doi.org/10.17804/2410-9908.2016.6.017-027>
23. A. V. Makarov, G. V. Samoylova, N. V. Gavrilov, A. S. Mamaev, A. L. Osintseva, T. E. Kurennykh, and R. A. Savrai, "Effect of preliminary nanostructuring frictional treatment on the efficiency of nitriding of metastable austenitic steel in electron beam plasma," *AIP Conf. Proc.* **1915**, 30011 (2017).
<https://doi.org/10.1063/1.5017331>
24. A. V. Makarov, N. V. Gavrilov, G. V. Samoiloa, A. S. Mamaev, A. L. Osintseva, and R. A. Savrai, "Effect of a continuous and gas-cyclic plasma nitriding on the quality of nanostructured austenitic stainless steel," *Obrab. Met. (Tekhnol., Oborud., Instrum.)*, No. 2, 55–66 (2017).
<https://doi.org/10.17212/1994-6309-2017-2-55-66>
25. M. R. Menezes, C. Godoy, V. T. L. Buono, M. Schwartzman, and J. C. Avelar-Batista Wilson, "Effect of shot peening and treatment temperature on wear and corrosion resistance of sequentially plasma treated AISI 316L steel," *Surf. Coat. Technol.* **309**, 651–662 (2017).
<https://doi.org/10.1016/j.surfcoat.2016.12.037>
26. A. V. Makarov, G. V. Samoiloa, N. V. Gavrilov, A. S. Mamaev, A. L. Osintseva, and R. A. Savrai, "The influence of preliminary deformation treatment on the hardening and quality of the nitrided surface of austenitic stainless steel," *Vektor Nauki Tol'yattinskogo Gos. Univ.*, No. 4, 67–74 (2017).
<https://doi.org/10.18323/2073-5073-2017-4-67-74>
27. Liu Zh., Ya. Peng, Ch. Chen, J. Gong, and Yo. Jiang, "Effect of surface nanocrystallization on low-temperature gas carburization for AISI 316L austenitic stainless steel," *Int. J. Pressure Vessels Piping*, **104053** (2020).
<https://doi.org/10.1016/j.ijpvp.2020.104053>
28. I. S. Zhidkov, A. I. Kukhareno, A. V. Makarov, R. A. Savrai, N. V. Gavrilov, S. O. Cholakh, and E. Z. Kurmaev, "XPS characterization of surface layers of stainless steel nitrided in electron beam plasma at low temperature," *Surf. Coat. Technol.* **386**, 125492 (2020).
<https://doi.org/10.1016/j.surfcoat.2020.125492>
29. Ya. Lu, D. Li, H. Ma, X. Liu, M. Wu, and J. Hu, "Enhanced plasma nitriding efficiency and properties by severe plastic deformation pretreatment for 316L austenitic stainless steel," *J. Mater. Res. Technol.* **15**, 1742–1746 (2021).
<https://doi.org/10.1016/j.jmrt.2021.08.082>
30. R. A. Savrai, P. A. Skorynina, A. V. Makarov, and A. L. Osintseva, "Effect of liquid carburizing at lowered temperature on the micromechanical characteristics of metastable austenitic steel," *Phys. Met. Metallogr.* **121**, 1015–1020 (2020).
<https://doi.org/10.1134/S0031918X20100105>
31. R. A. Savrai and P. A. Skorynina, "Structural-phase transformations and changes in the properties of AISI 321 stainless steel induced by liquid carburizing at low temperature," *Surf. Coat. Technol.* **443**, 128613 (2022).
<https://doi.org/10.1016/j.surfcoat.2022.128613>
32. M. L. Bernshtein and A. G. Rakhshadt, *Metallography and Heat Treatment of Steel: Reference Book* (Metallurgiya, Moscow, 1983).

Translated by N. Podymova